Spore number control and breeding in *Saccharomyces cerevisiae*: a key role for a self-organizing system

Christof Taxis, Philipp Keller, Zaharoula Kavagiou, Lars Juhl Jensen, Julien Colombelli, Peer Bork, Ernst H.K. Stelzer, and Michael Knop

The European Molecular Biology Laboratory, D-69117 Heidelberg, Germany

Spindle pole bodies (SPBs) provide a structural basis for genome inheritance and spore formation during meiosis in yeast. Upon carbon source limitation during sporulation, the number of haploid spores formed per cell is reduced. We show that precise spore number control (SNC) fulfills two functions. SNC maximizes the production of spores (1–4) that are formed by a single cell. This is regulated by the concentration of three structural meiotic SPB components, which is dependent on available amounts of carbon source. Using experiments and computer simulation, we show that the molecular mechanism relies on a self-organizing system, which is able to generate particular patterns (different numbers of spores) in dependency on one single stimulus (gradually increasing amounts of SPB constituents). We also show that SNC enhances intratetrad mating, whereby maximal amounts of germinated spores are able to return to a diploid lifestyle without intermediary mitotic division. This is beneficial for the immediate fitness of the population of postmeiotic cells.

Introduction

The ability to respond to environmental conditions is essential for cells. The proper response is generated upon the integration of cues that are provided by the external situation as well as the internal state and determines the future behavior of the cells (Schneper et al., 2004). Meiosis and sporulation in the budding yeast *Saccharomyces cerevisiae* is a well-studied example. It is induced by deprivation of nitrogen and fermentable carbon sources and requires diploidy. A specific developmental program executed during meiosis generates the tetrad containing four spores, each of which harbors a haploid genome (Kassir et al., 2003). Spore assembly takes place within the mother cell, which matures at the end of the process to the ascus membrane that keeps the spores together. Spore formation starts at the beginning of meiosis II with the assembly of new spore plasma membranes, the so-called prospore membranes (PSMs). This process, although equivalent to formation of the bud in mitotic cells, is regulated entirely differently. PSM assembly takes place at the spindle pole bodies (SPBs; the fungal centrosomes), which are modified for this purpose with a meiosis-specific structure, the meiotic plaque (MP). The MP is composed of three essential components: Mpc54p, Mpc70p, and Spo74p (Knop and Strasser, 2000; Bajgier et al., 2001; Nickas et al., 2003). Vesicles of homogeneous size (60–70 nm) align before PSM assembly on top of the MP (Knop et al., 2005; Riedel et al., 2005). If one MP component is absent, the MP structure does not form. Vesicle binding to the SPB still occurs, although their assembly into a PSM is blocked (Moreno-Borchart and Knop, 2003; Taxis and Knop, 2004). Initiation of PSM formation via fusion of the vesicles leads to the formation of a new membrane system. During the course of meiosis II, the PSMs resemble flattened pouches. Each of them grows around a nuclear lobe into which a haploid genome becomes segregated. Nuclear fission takes place before postmeiotic cytokinesis, when the PSMs close up. This generates four new compartments: the prospores, which are surrounded by two lipid bilayers that result from PSM closure. Subsequent deposition of large amounts of spore wall material between these membranes leads to formation of the spore walls. This results in an ascus containing four mature spores (Shimoda, 2004). Interestingly, if adverse conditions are imposed during sporulation, such as heat or limitation of the carbon source, the cells respond to these conditions by the production of an increased number of asci frequently containing two instead of four haploid spores (Davidow et al., 1980; Okamoto and Iino, 1981). This is the consequence of the involvement of only one SPB per meiosis II

Correspondence to Michael Knop: knop@embl.de

Abbreviations used in this paper: CP, central plaque; MP, meiotic plaque; PSM, prospore membrane; SNC, spore number control; SPB, spindle pole body.

The online version of this article contains supplemental material.

The Journal of Cell Biology, Vol. 171, No. 4, November 21, 2005 627–640
http://www.jcb.org/cgi/doi/10.1083/jcb.200507168

Supplemental Material can be found at:
http://www.jcb.org/cgi/content/full/jcb.200507168/DC1

spindle in the assembly of a spore (Davidow et al., 1980; Okamoto and Iino, 1981; Ishihara et al., 2001; Wesp et al., 2001; Nickas et al., 2003, 2004). In dyads, the two haploid genomes packaged into spores are segregated during meiosis I (nonsister genomes). SPB duplication in *S. cerevisiae* is conservative (Adams and Kilmartin, 1999). Recently, it has been shown that the specific SPBs involved in spore formation in dyads are the newer ones that were formed directly before meiosis II (Nickas et al., 2004). In the same study, it was demonstrated that the regulation of dyad formation relies on the production of an intermediate metabolite by the glyoxylate pathway. It was argued that a sensing system is able to impose specific regulation of either the two new or the two old SPBs in order to achieve dyad formation.

In this study, we provide an in-depth analysis of the molecular mechanism underlying regulated dyad formation. We demonstrate that the formation of any number of spores (1–4) is subject to regulation in accordance to the nutritional situation of the cell. We describe a new molecular mechanism based on a self-organizing system, which regulates the meiotic SPB function toward spore formation. It provides sporulating cells with a simple way to maximize the number of formed spores. We termed this regulation spore number control (SNC).

Automixis, which is the mating of spores from the same ascus, has been observed occasionally for yeast (Guilliermond, 1905; Winge and Laustsen, 1937). We show that mating of germinating spores occurs with high frequency and mostly involves mating between spores of nonsister origin. We demonstrate that SNC ensures this rate is held constant on the population level over a broad range of sporulation conditions. This ensures the transmission of a constant and high degree of paternal heterozygosity through the meiotic division. We provide indications that this ability is associated with two types of advantages: masking of haploid lethal mutations and enhanced mean fitness of the postmeiotic generation.

Results

MP formation is rate limiting for spore formation

The MP is a prominent addition to the SPB, which specifically appears in meiosis II. It is essential for spore formation because of its function as a scaffold for the assembly of the plasma membranes of spores. It has been suggested that one way to regulate the number of spores would be via assembly of less than four MPs; however, attempts to quantitatively correlate these two measures failed (Davidow et al., 1980). To identify the rate-limiting step, we used GFP fused to one of the structural components of the MP (Mpc54p) to quantitatively address the number of MPs assembled per cell (Fig. 1 B) and to correlate them with the number of spores formed at the end of sporulation (Fig. 1 A). We analyzed the number of MPs present in populations of cells during different time points of a synchronous sporulation experiment. Cells were sporulated in the presence of low levels of acetate in the medium, which leads to the formation of many dyads. We found a negative correlation with time and the number of assembled MPs: cells undergoing MP

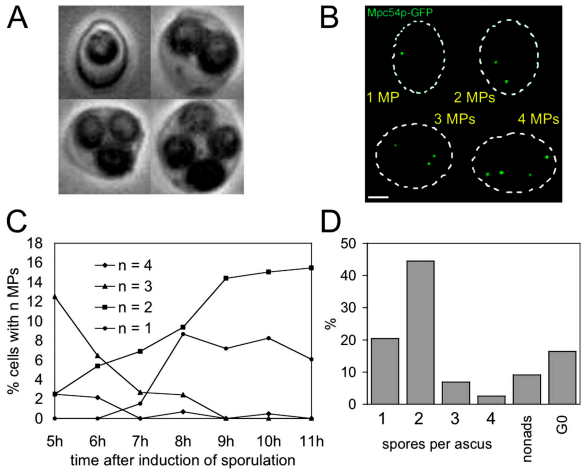

Figure 1. **Tight SNC in budding yeast meiosis is correlated with MP assembly.** (A) Examples of sporulated yeast cells (asci) with different numbers of spores. (B) Examples of cells with 1–4 meiotic plaques (MPs) visualized using a fully functional Mpc54p-GFP fusion (yeast strain YCT730; Knop and Strasser, 2000). Bar, 2 μm. (C) Occurrence of cells with different numbers of MPs during a meiotic time course experiment. Sporulation was performed using 0.015% acetate. (D) Composition of the culture of C after 36 h of sporulation. Spores were counted as described in Materials and methods. Nonads = meiosis but no spores.

assembly early in the time course produced more MPs and vice versa (Fig. 1 C). This explains the lack of correlation that was observed by Davidow et al. (1980), because they investigated the situation at one time point during sporulation (by electron microscopy) and compared it with the numbers of spores produced at the end. Taking this change of population composition into consideration, MP formation and the composition of the cell culture with respect to spore number distribution (Fig. 1 D) correlates well. Additionally, we stained the cells with Hoechst 33342 at each time point during the time course. This revealed that all of the cells undergoing meiosis completed meiosis II and separated their genomes even if the cells formed less than four spores. After completion of sporulation, DNA that was not incorporated into a spore was not detected anymore (unpublished data).

Metabolic control regulates the protein levels of MP components

It has been shown that changed levels of the genes encoding for the MP components Mpc54p, Mpc70p, and Spo74p influence the ratio of dyads versus tetrads: lower expression yields more dyads and vice versa (Bajgier et al., 2001; Wesp et al., 2001; Nickas et al., 2003). To analyze this phenomenon quantitatively, we constructed strains with discrete changes of the gene dosage of MP genes: one, two, and four copies of all three genes each. This revealed a strict correlation of the amounts of spores obtained in populations of sporulating cells with the gene dosage (Fig. 2 A). Reduction of the amounts of acetate available to the sporulating cells reduced the amounts of formed spores (Fig. 2 B). This was a result of a corresponding lowered amount of MP components, as shown by Western blotting (Fig. 2 C). Together, the results in Figs. 1 and 2 show that MP formation is the rate-limiting factor that determines the

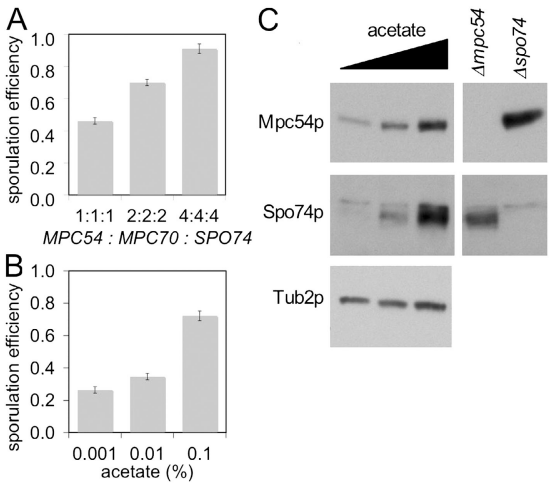

Figure 2. **Acetate-dependent regulation of sporulation efficiency occurs via regulation of the amounts of MP components.** (A) Sporulation efficiency depends on the dosage of genes encoding for MP components. (B) Sporulation efficiency (1.0–100%) depends on the amount of externally provided acetate. (A and B) Error bars indicate the SD (three experiments). (C) Immunoblot analysis of Mpc54p, Spo74p, and tubulin (as a loading control). The black triangle denotes increasing amounts of KAc (0.001, 0.01, and 0.1% acetate). The samples used for immunoblotting were cell lysates derived from pooled aliquots of the sporulation cultures taken at regular intervals during a time course (4, 5, 6, 7, 8, 10, and 12 h) of wild-type cells. Therefore, the detected amounts of Mpc54p and Spo74p roughly represent the integrated amounts of totally produced protein.

number of spores formed. Furthermore, the experiments show that the amount of MP components is controlled by available external energy (acetate) and that this determines the number of spores formed.

Live cell imaging of MP assembly

The results indicate that MP formation includes a mechanism to translate gradually increasing amounts of MP components into a digitized output of one to four assembled MPs. To address this mechanism in detail, we performed live cell imaging using the Mpc54p-GFP fusion. To indicate the age of the SPBs, the SPB component Spc42p was fused to RFP with retarded maturation of the chromophore. Therefore, only the two older SPBs show a red fluorescence. These two SPBs can be distinguished by the brightness of the signal, with the oldest SPB having the brightest signal. Fig. 3 A shows the transition from anaphase meiosis I to metaphase meiosis II in a typical cell that assembled four MPs. This revealed cytoplasmic as well as SPB-localized Mpc54p-GFP during meiosis I. With entry into meiosis II, four Mpc54p-GFP dots appeared and increased quickly in brightness, whereas the cytoplasmic Mpc54p-GFP signal decreased. We frequently saw that the MP at the oldest SPB was assembled with a delay of several minutes relative to the other SPBs (see Fig. 3 B for quantification). Moreover, we observed cells that assembled only three MPs (Fig. 3 C; quantification shown in D). In this case, the third MP was assembled with a delay (at the second oldest SPB). The signal at the oldest SPB never progressed above the very faint signal seen in meiosis I and early in meiosis II. We were unable to record cells that assembled only two MPs, as the amount of Mpc54-GFP in these cells appeared to be much lower than in the cells that assembled three or four MPs. This is in accordance with a decrease of Mpc54p abundance in cell populations undergoing sporulation at low levels of KAc (Fig. 2 C). The live cell imaging experiments indicate a difference between the SPBs, which leads to differences in the time needed to assemble individual MPs and the amount of MP components necessary to assemble MPs at specific SPBs.

The use of Spc42p-RFP as an aging marker revealed that young SPBs (without fully matured RFP) are preferred (Fig. 3, A and C). In one sample with three MPs, however, we noticed that the oldest and not the second oldest SPB acquired an MP (not depicted). Thus, the rule of "new SPBs first" appears to not always apply. This prompted us to address the fidelity of the age bias for SPB selection on a statistically significant level. We set up a system that allowed faithful discrimination of all four SPBs based on their age (four SPBs of three different generations: two new, one intermediate, and one oldest SPB; Fig. 3 E) and analyzed their likelihoods to assemble MPs in situations in which one, two, or three MPs were assembled. This revealed that when one MP was assembled, one of the new SPBs was always selected. When two MPs were assembled, both MPs were on the new SPBs 96% of the time, and one of the new SPBs and the intermediate SPB acquired an MP 4% of the time. For cells with three MPs, 99% assembled MPs on the three newer SPBs, and in 1% of the cells, the oldest instead of the intermediate SPB acquired an MP (Fig. 3 F). These results were independent of the energy available to the sporulating cells and the gene dosage of MP component genes (unpublished data). Together, this indicates that SPB selection involves stochastic processes that direct MP formation with a certain likelihood to newer SPBs.

The MP resembles a crystal

The rapid relocalization of cytoplasmic Mpc54p-GFP signal to SPBs coincides with the appearance of bright Mpc54p-GFP–labeled MPs inside the cell and the transition of meiosis I to meiosis II. This suggests that the formation of MPs is cell cycle controlled. We used FRAP to investigate the exchange rate of Mpc54p-GFP between the SPBs and the cytoplasm in cells before assembly of MPs (before and during meiosis I) and in cells with assembled MPs (during meiosis II). For cells before and during meiosis I, we found that Mpc54p-GFP exchanged completely within a time span of ~30 s (Fig. 4 A). In cells in meiosis II, however, the exchange of Mpc54p-GFP between the SPB and cytoplasm was very low (Fig. 4 B). We made use of *Δmpc70* cells to directly test the influence of the cell cycle stage on the exchange rate of Mpc54p-GFP. Binding of Mpc54p to the SPB is not impaired in these cells, but MP assembly is blocked as a result of the deletion of one MP component (Knop and Strasser, 2000). FRAP measurements revealed that in *Δmpc70* cells, Mpc54p-GFP exchanged within ~30 s in meiosis II (Fig. 4 C). In addition, the cytoplasmic amounts of Mpc54p-GFP remained high in these cells. This indicates that the cell cycle stage does not, per se, influence the binding of Mpc54p-GFP to the SPB but influences the formation of a fully functional MP.

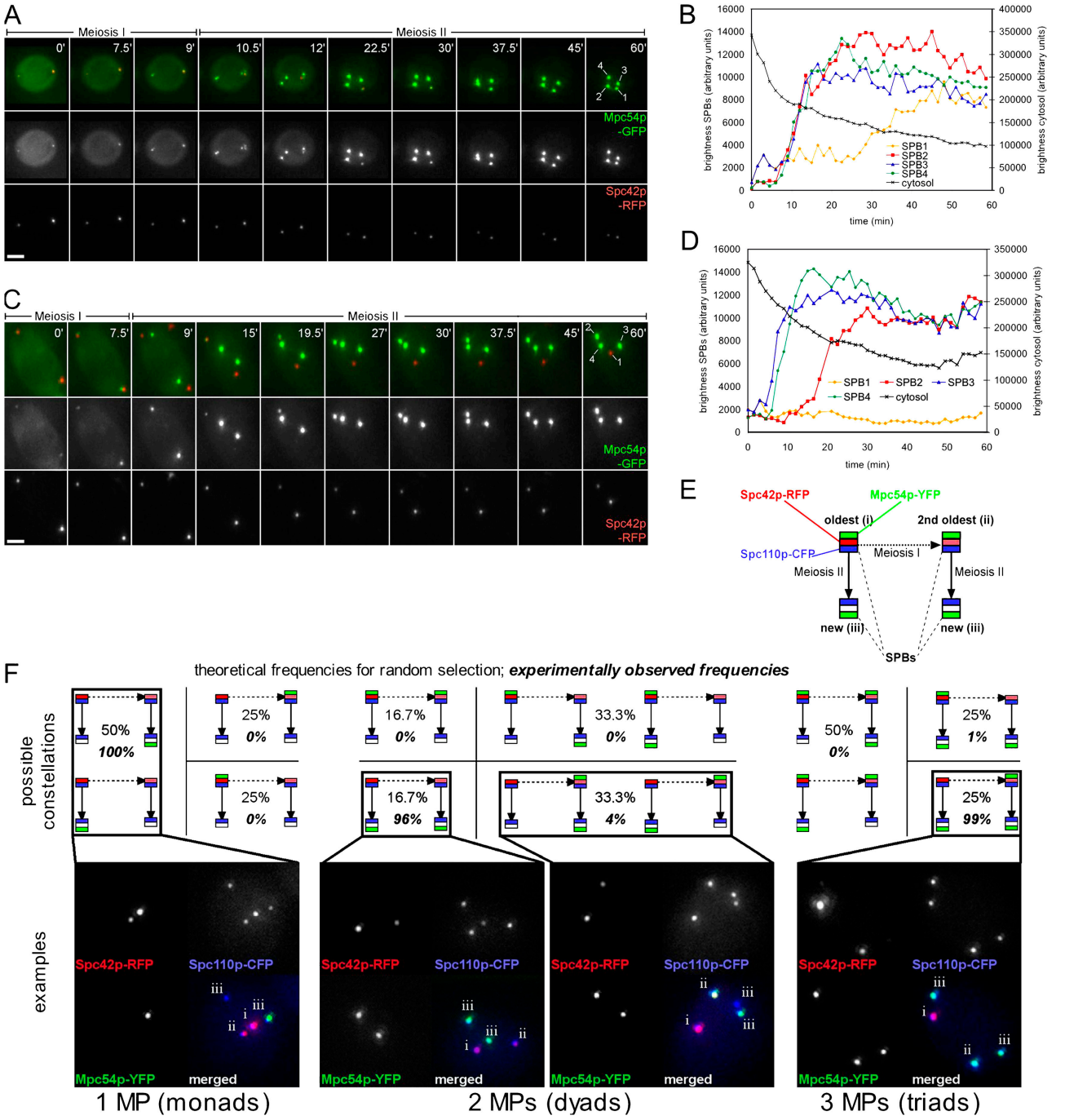

Figure 3. **Dynamics of MP assembly and stochastic SPB selection.** (A) Live cell imaging of a cell that forms four MPs and (C) of a cell that forms three MPs. MPs were visualized using Mpc54p-GFP, whereas Spc42p-RFP was used to label old SPBs. Selected frames (maximum projections) at the indicated time points after the start of recording are shown. Time is given in minutes. Bars, 2 μm. The full videos are provided as Videos 1 and 2, available at http://www.jcb.org/cgi/content/full/jcb.200507168/DC1. (B) Quantification of cytoplasmic- and SPB-localized Mpc54p-GFP fluorescence intensity from A. The numbering of the SPBs corresponds to the numbering shown in the last frame of the video snapshots depicted in A. (D) Quantification (see B) of C. (E) SPBs of three different generations are present in meiosis II. The cartoon outlines the relationship of SPBs and fluorescent protein labels used for the experiment shown in F. Arrows indicate duplication of SPBs during meiosis I (dashed arrow) and meiosis II (normal arrows). MPs were visualized using Mpc54p-YFP (green signals) and the position of all SPBs using CFP fused to the inner plaque protein Spc110p (blue signals; Kilmartin et al., 1993). Old and new SPBs were discriminated based on the signal brightness of a fluorescent timer (RedStar/RFP; Knop et al., 2002) fused to the integral SPB component Spc42p (Donaldson and Kilmartin, 1996). This allows that SPBs from three different generations can be distinguished and that the age of the SPBs can be correlated with the assembly of MPs. (F) Distribution of MPs to SPBs from different generations in cells with different numbers of MPs. The pictograms show all theoretically possible constellations for the situation with one, two, or three MPs per cell. Pictograms for constellations that are indistinguishable by the used method are grouped together. The microscopic pictures show representative cells for selected cases. The oldest SPB (i) is marked with the brightest RFP signal, and the intermediate SPB (ii) is marked with the second brightest RFP signal. The position of the two new SPBs (iii) is indicated by the CFP label, whereas they are not or are only faintly labeled with the RFP marker. The percentage of occurrence of the different possible constellations that can be distinguished by this method as well as the theoretical random distribution are indicated. Yeast strain YCT806 was used for this experiment. 299 cells were evaluated.

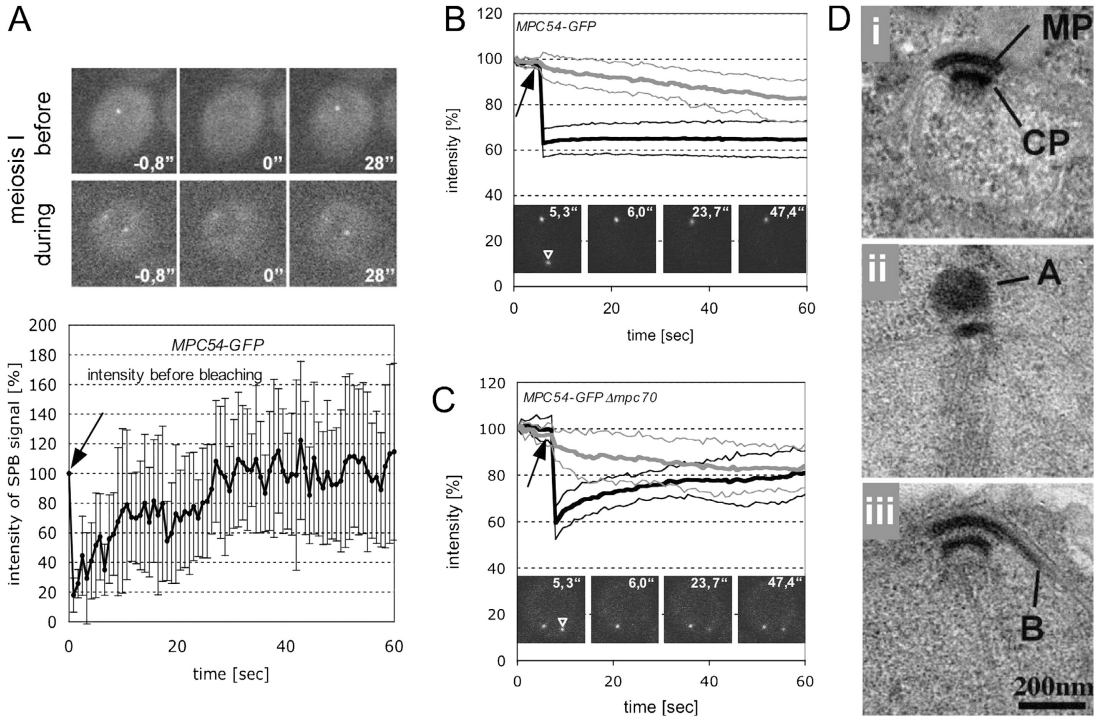

Figure 4. **MP assembly is associated with crystal assembly at the SPBs in meiosis II.** (A) FRAP analysis of Mpc54p-GFP in cells before and during meiosis I. The pictures show selected frames from a cell before meiosis I and a cell during meiosis I (as indicated). The plot represents an average of six experiments; error bars depict the SD. Time is indicated in seconds. The arrow indicates the time point of bleaching. (B) FRAP analysis of the binding of Mpc54p-GFP components to SPBs in wild-type cells in meiosis II. The plots represent averages of nine experiments. For quantification, each individual recording was normalized to 100% brightness for the time point 0. The thick black line represents the average signal from bleached SPBs, whereas the thick gray line represents the average signal from unbleached SPBs, which served as internal controls. Thin lines in the corresponding colors show the SDs. The arrow indicates the time point of bleaching. Frames from representative experiments at indicated time points after the start of the recording are shown. The first frame shows the situation just before photobleaching. Time is given in seconds. The arrowhead points to the SPB that was bleached. (C) Same as in B but using a *Δmpc70* mutant. Please note that the experiments shown in A were performed on a different microscope than the experiments shown in B and C (see Materials and methods for details). (D) Structure of the MP in a wild-type cell in meiosis II (i) and upon simultaneous overexpression of Mpc54p, Mpc70p, and Spo74p in a cell in meiosis I (ii) or meiosis II (iii). A, amorphous structure at the cytoplasmic side of the SPB; B, lateral extension of the MP.

What is the difference between an SPB that can exchange Mpc54p-GFP and one that cannot? The assembled MP has a high similarity to the central plaque (CP) of the SPB (Fig. 4 D, i) when observed by electron microscopy. Lateral extension of the CP was demonstrated upon overexpression of its core constituent Spc42p (Donaldson and Kilmartin, 1996). Based on cryoelectron microscopy performed with isolated SPBs, it was shown that the CP has a crystal-like structure with a hexagonal package (Bullitt et al., 1997). We used the strong and inducible *CUP1* promoter to up-regulate all three MP components simultaneously to address whether lateral expansion of the MP can be induced as well. This led to the formation of large, amorphous protein aggregates at the SPBs for cells in meiosis I (Fig. 4 D, ii). However, cells in meiosis II exhibited lateral enlargement of the MPs (Fig. 4 D, iii). This result demonstrates that only assembled MPs allow binding of new components specifically to their lateral sides. This suggests that the MP, which is analogous to the CP, has a crystal-like protein structure. Thus, this property may explain the irreversible incorporation of subunits in assembled MPs. Together, our results suggest a simple molecular mechanism based on crystal formation on individual SPBs (Fig. 5 A) and competition between the different crystals for subunits (Fig. 5 B) that enables digitization of graded amounts of available MP components into discrete numbers of SPBs with MPs (see Discussion).

Simulation of SNC in wild-type and mutant cells

The acetate-dependent regulation of available MP components and the mechanism of MP assembly provide a simple way to connect the available external energy to the number of spores a cell produces. Each individual cell within a population decides on its own how many spores it can form, which gives rise to mixed populations. To quantitatively study SNC that is dependent on increasing amounts of acetate, we performed dose–response analysis (experimental setup outlined in Fig. 6 A). This sporulation profile revealed strict dependency of the composition of the sporulated cell populations on external acetate concentrations (Fig. 6 B). At very low acetate concentrations, mostly monads were formed, whereas with increasing acetate, first dyads and later triads became prominent, finally followed by tetrads. Furthermore, we noticed the formation of a few nonads (which equals meiosis but no spores) at a very low acetate concentration. The total amount of formed spores (sporulation efficiency) strongly increased with available acetate between concentrations of 0 and 0.04%. Above this concentration, the sporulation efficiency increased much more slowly. There might be at least two reasons for this: a nonlinear correlation between acetate and the amounts of MP components or saturation, as no cell is able to assemble more than

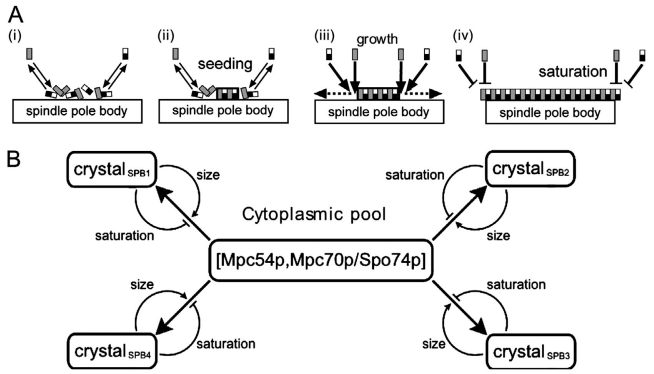

Figure 5. **Self-organization and feedback during MP assembly.** (A) Schematic model for the formation of an MP. Gray rectangles represent Mpc54p, and black/white rectangles represent heterodimers formed from the association of Mpc70p with Spo74p. Black-bordered arrays of Mpc54p/Mpc70p/Spo74p represent crystals. The size of an arrow indicates the relative on or off rates of MP components during the amorphous phase or after initiation of MP assembly during crystal growth. Dashed arrows indicate the directions of crystal growth. (B) Flow chart for MP assembly at different SPBs from a cytoplasmic pool of MP components.

four spores. During the whole experiment, the induction of meiosis was not, per se, significantly influenced by different amounts of acetate present in the medium, as can be seen from constant amounts of cells not undergoing meiosis (Fig. 6 B, G_o cells). The sporulation profile results from the sum of individual cellular responses to available acetate. It is a precise measure of all factors that together regulate SNC. Thus, it provides an ideal base to study different aspects of SNC using one type of assay. We used computer simulation in order to address the different aspects that together make up the sporulation profile. The simulation contained three parts. These are the digitization module that converts a graded increase in available MP components into a digital output (Fig. 6 C) and two parts that relate to the translation of acetate into amounts of MP components (acetate → protein function; Fig. 6 D) and to population statistics (Fig. 6 E and supplemental material, available at http://www.jcb.org/cgi/content/full/jcb.200507168/DC1).

The simulation was sufficient to reproduce the characteristics of the experimentally determined sporulation profile of the wild-type strain (Fig. 6 F). A realistic simulation should be able to reproduce the sporulation profiles of mutants that affect specific parameters of the simulation upon adjustments of the affected parameters. For this analysis, we used the MP gene dosage mutants with well-known and discrete disturbances of the SNC system (Fig. 2 A). In these mutants, it is predicted that only the average amplitude of the acetate → protein function is changed, but not its shape (Fig. 6 D). This resulted in simulated sporulation profiles that reproduced the experimentally obtained mutant profiles very well (Fig. 6, G and H). The parameters and distributions used for the wild type and their values in the mutants are shown in Fig. 6 E. Next, we applied the simulation to analyze the *Δady2* mutant, which predominantly forms dyads (Rabitsch et al., 2001). Ady2p is a conserved protein that is expressed upon the induction of meiosis and localizes to the plasma and vacuolar membranes in meiotic cells (unpublished data). It contains several transmembrane domains. Its function is not yet clarified because it has been implicated in a multitude of processes; among them is the regulation or direct uptake of acetate but not growth on acetate (Paiva et al., 2004) and the secretion of ammonium (Palkova et al., 2002). The sporulation profile of the *Δady2* mutant revealed that the composition of sporulated cultures is independent on external acetate (Fig. 6 I). According to the simulation, this can most easily be achieved by changing the acetate → protein function to a block function (Fig. 6 D). In this case, the amounts of MP components should be independent of external acetate, which was indeed the case (Fig. 6 K). Upon the addition of extra copies of MP genes, increased numbers of spores should be formed, but the composition of the sporulated populations should still be independent of acetate. This proved to be true (Fig. 6 J). The intersection of the acetate → protein functions of the wild-type and corresponding *Δady2* mutant strain revealed that constitutive MP gene expression corresponds to an apparent acetate concentration of 0.01% in the wild-type strain (Fig. 6 D). Translated into a biological interpretation, this result indicates that Ady2p is required for up-regulation and down-regulation of MP component levels in a dependency on external acetate. Very similar results were obtained using the *Δady2* mutant with extra copies of the MP genes and the corresponding wild type (with additional MP gene copies; Fig. 6, H and J). Together, these results support the usefulness of the model and demonstrate its application for the understanding of unknown mutants.

SNC is optimized for providing maximal amounts of mating partners within the ascus

In *S. cerevisiae*, the mating type locus (*MAT*) is linked to the centromere of chromosome III (*CEN3*; Hawthorne and Mortimer, 1960). The *MAT-CEN* linkage causes the spores in nonsister dyads to be of opposite mating types. The frequency of this behavior depends on two factors: the fidelity of nonsister encapsulation in dyads and the genetic *MAT-CEN* linkage. The fidelity with which dyads contain nonsister spores is 96% irrespective of the acetate concentration used for the experiment and independent of the *Δady2* mutation (unpublished data). The ability to form dyads that contain spores of opposite mating types suggests that yeast spores are able to undergo direct mating upon germination, which has been reported many years ago (Guilliermond, 1905; Winge and Laustsen, 1937). Dyads as well as triads can theoretically form one diploid cell upon the mating of spores, and tetrads can form two (Fig. 7 A). We used the asci compositions of sporulated wild-type cells as revealed by the sporulation profile (Fig. 6 B) to calculate the amounts of diploids that could be formed via intratetrad spore–spore mating. As shown in Fig. 7 B, the SNC mechanism enhances this number especially in poor sporulation conditions. Notably, this requires the *MAT-CEN* linkage and the spores in dyads to be nonsister (Fig. 7 B).

To validate this prediction experimentally, we designed a tester strain. We integrated different dominant markers, each directly next to the centromere on one of the homologous chromosomes V (diploid strain). Upon sporulation, direct mating of nonsister spores from the same ascus should reconstitute the

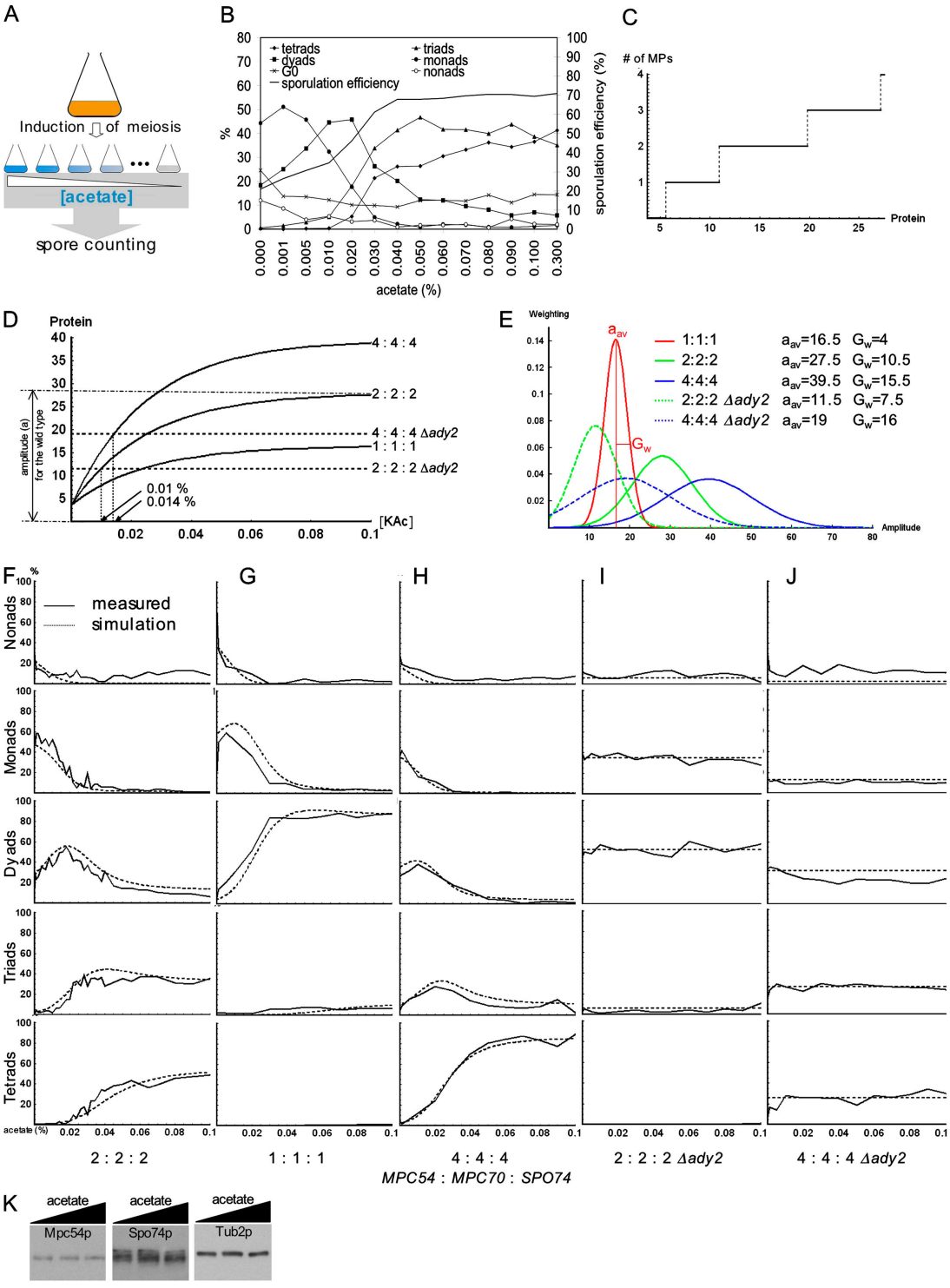

Figure 6. **Predictive simulation of SNC in cell populations and experimental validation of the model.** (A) Outline of the experimental setup. Aliquots of cells grown on presporulation medium were induced to undergo meiosis in the presence of different amounts of acetate. Spores were counted after completion of sporulation (~36 h). (B) Sporulation profile of the wild-type strain (YKS32). The occurrences of six different species (G_o cells [no induction of meiosis], nonads [meiosis, but no spores], monads, dyads, triads, and tetrads) are plotted as a function of acetate in the medium. The sporulation efficiency indicates the integrated amounts of produced spores (100% sporulation efficiency: all cells form tetrads). (C) Example for the output of the digitization module. (D) Acetate → protein functions of various strains (as indicated). The amplitude of the functions corresponds to the values for acetate → ∝. (E) Population statistics using a Gaussian distribution (defined by the parameters a_{av} and G_w) that describes cellular differences of the different strains in response to acetate (see supplemental material). (F–J) Measured and simulated sporulation profiles of different strains (as indicated). Superimpositions of the simulated and measured curves for the different species are shown. Please note that all simulations were fitted to sporulation profiles obtained from individual experiments. For the wild-type strain (I), one experiment with a high resolution (34 acetate concentrations) was used in order to provide an excellent database to calibrate the model. (K) Western blot revealing acetate-independent expression of MP components in the *Δady2* mutant (sporulation profile shown in I; see Fig. 2 C for experimental conditions; the blots shown here can be directly compared with the blots shown in Fig. 2 C). Supplemental material is available at http://www.jcb.org/cgi/content/full/jcb.200507168/DC1.

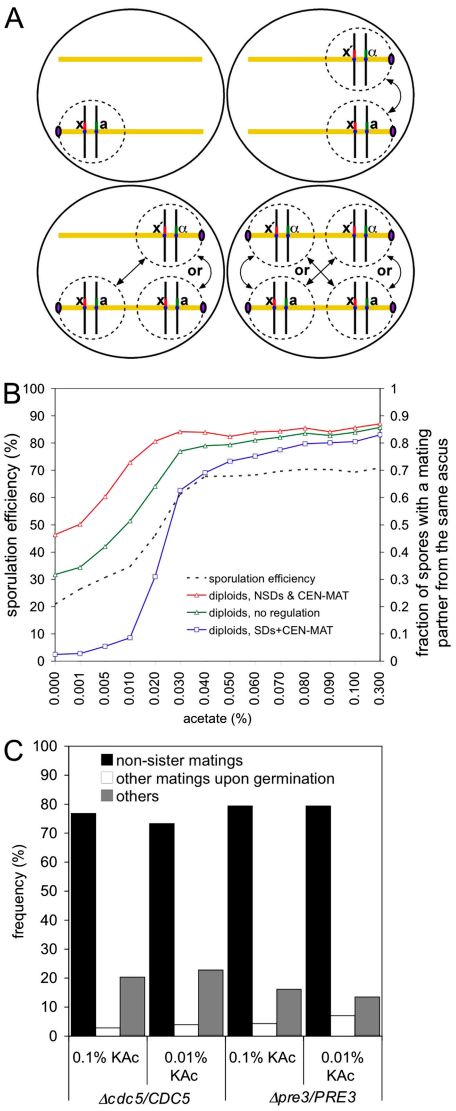

Figure 7. **Mating between nonsister spores in *S. cerevisiae*.** (A) The cartoon illustrates the possible intratetrad mating events in dyads, triads, and tetrads. In dyads, one haploid genome per meiosis II spindle (yellow line) becomes aborted, which results in the formation of two spores (dashed line) containing nonsister genomes. As a result of the centromere linkage of the mating-type locus (*MAT*; a or α) in *S. cerevisiae*, the heterozygous situation of any centromere-linked allele (x or x′) will be preserved in the diploid cell that is formed upon mating. (B) Theoretical frequency of diploids formed by mating of spores from the same ascus in dependency on *MAT-CEN* linkage and nonsister dyad (NSD) formation. The frequency was calculated based on the sporulation profile of the wild-type strain (Fig. 6 B). Tetrads were assumed to form two diploid cells, and triads were assumed to form one. Dyads formed one diploid cell at a rate of 100% if they were of nonsister origin, at a rate of 66.6% if they were of random origin, and at a rate of 0% if they were of sister origin (sister dyads, SDs). (C) Mating between spores assayed in populations of asci. Two different populations of asci, obtained under high acetate or low acetate sporulation conditions, were used for this experiment. The asci (10^7) were allowed to germinate (after killing of nonsporulated cells) on rich medium. The formed populations of diploid cells were assayed for different types of mating events.

heterozygous state of this locus. To exclude mitotic divisions before mating, we deleted one copy of mitotically essential genes—either *PRE3* (a proteasomal subunit) or *CDC5* (polo kinase). Both genes are located directly next to a centromere, and nonsister mating should restore the heterozygous state of this locus. To mimic natural yeast cells, we used a homothallic strain in which haploid cells (but not spores; Herskowitz, 1988) can change the mating type. We analyzed populations of asci after growth on rich medium for 24 h for the formation of diploid cells containing all three markers simultaneously. We found that all cells were diploids, and 75–80% contained all three markers (Fig. 7 C), which indicates that the heterozygous situation of the parental strain was maintained at these loci. As predicted (Fig. 7 B), this frequency was independent of the acetate concentration present during sporulation. This emphasizes the important role of SNC to enable high frequency of intratetrad mating under a variety of sporulation conditions.

Possible influence of intratetrad mating on genome organization and fitness

Our experiments with the heterozygous *Δcdc5* and *Δpre3* mutants (Fig. 7 C) demonstrate clearly that spores that have haploid lethal mutations in their genomes are still able to mate efficiently. The fidelity of rescuing a lethal mutation depends on its linkage to the *MAT* locus, as it is the only locus where heterozygosity is reconstituted 100% of the time upon mating of spores from the same ascus. For non-*MAT*–linked loci, the heterozygous state is preserved 66.6% of the time, whereas for *MAT*-linked loci, this value falls between 66.6% and 100% depending on the strength of the linkage (Zakharov, 1968; Kirby, 1984). In the case in which the *MAT* locus is linked to a centromere, as in *S. cerevisiae*, linkage to the *MAT* locus is expanded to all other centromere-linked sequences in the genome (Fig. 7 A). We calculated the fraction of the yeast genome that exhibits genetic linkage to the mating-type locus based on the genetic map of yeast (www.yeastgenome.org) and found it to be roughly 25% of the yeast genome (~1,440 of the 5,792 genes; see Materials and methods). Moreover, masking of heterozygous deleterious mutations upon mating of spores from the same ascus would be particularly effective if mitotically essential genes exhibited centromere linkage. This idea prompted us to analyze the genome-wide distribution of all essential genes of *S. cerevisiae*. We found a significant bias for their localization in centromere-adjacent regions (Fig. 8 A).

Preservation of a heterozygous state may also be associated with an advantage in which a diploid genome is harboring heterozygosities that do not interfere with haploid growth itself. To test this, we constructed a hybrid diploid *S. cerevisiae* strain from two different yeast strains: one isolated from human patients (YJM145 background; McCusker et al., 1994) and one isolated from a vineyard (SK-1; Kane and Roth, 1974). Both yeast strains are able to undergo mating-type switching (homothallic strains) and show a spore viability close to 100%, suggesting that they contain no haploid lethal heterozygosities in the genome. From sporulated cultures of this strain, we generated two pools of diploids. We obtained one pool from single isolated spores, which gave rise to homozygous diploids upon outgrowth. We obtained the other pool from isolated dyads that produced diploids with maximal amounts of preserved heterozygosities. Using serial transfer, we compared the fitness of the two pools over a period of ~60 generations. This revealed that only 5% of the homozygous diploids exhibited a fitness

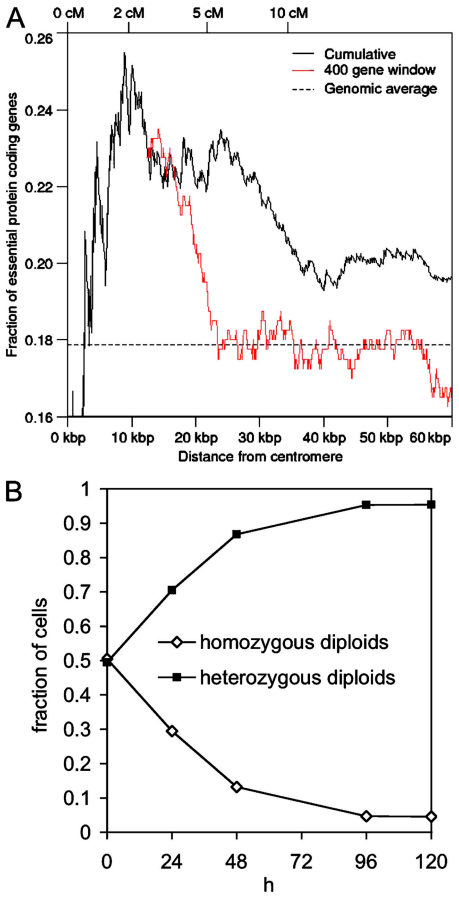

Figure 8. **Possible influence of intratetrad mating on genome organization and fitness.** (A) Clustering of essential genes near centromeres. Conversion of physical distance into genetic distance was performed using the published genetic map of the yeast genome (Cherry et al., 1997). Two different types of plots were performed to address the clustering: cumulative frequency of essential genes with increasing distance to the centromere (for all chromosomes simultaneously) and a window of 400 genes. This overrepresentation of essential genes is significant at a $P = 0.03$ according to a hypergeometric test. (B) Fitness comparison by serial dilution of heterozygous versus homozygous diploids obtained from sporulated cells of a heterozygous diploid strain. A 1:1 mixture of diploids formed from isolated dyads and diploids that were obtained from isolated spores was used for the fitness competition experiment over five growth periods of 24 h (total of ~60–65 generations).

that was comparable with the fitness of the heterozygous population (Fig. 8 B). Together, these results demonstrate that organization of the yeast genome enables the preservation of a high degree of heterozygosities upon intratetrad mating and that this is associated with an immediate fitness benefit.

Discussion

SNC and nonsister spore mating: biological significance

In this study, we analyzed the molecular mechanism that enables sporulating cells to regulate the formation of spores from one to four. The experiments clearly indicate that regulation is optimized to fulfill two functions: to exactly adjust spore production to situations with limiting amounts of available energy resources and to simultaneously produce maximal amounts of spores that are able to mate with a nonsister spore upon germination. A cell commits itself to form a certain number of spores at the beginning of meiosis II. The implementation of a regulatory mechanism at this step during meiosis is cost effective; it does not interfere with the inevitable processes that are needed to conduct meiosis (i.e., the meiotic divisions), but it effectively prevents wasting resources for the formation of too many spore intermediates. The regulatory mechanism generates maximal amounts of spores that mate with a nonsister spore from the same ascus directly after germination (Fig. 7, B and C). The regulatory mechanism includes the assembly of PSMs at selected SPBs and incorporation of one genome per meiosis II spindle in case of dyad formation. Another feature is the *MAT-CEN* linkage, which allows the mating of spores in a dyad. Mating of spores of the same ascus is inbreeding, and, if frequent for a given species, it is highly likely to have an impact on the population genetics of a species (Bell, 1982).

SNC allows the formation of a high number of diploids under different sporulation conditions through the mating of spores from the same ascus (Fig. 7). Our results demonstrate that the majority of *S. cerevisiae* spores indeed mate directly upon germination and, thus, return to a diploid lifestyle without any haploid mitotic divisions. Being a diploid species offers a number of advantages that are associated with having two copies of each gene present in the genome. Cells are less sensitive to mutagenic conditions (Mable and Otto, 2001), and adaptive evolution may be accelerated by the ability to preserve allelic variations or different genetic traits in the genome. For acquisition of new advantageous mutations, diploidy is a disadvantage, but only in the context of large populations in the absence of meiosis (Zeyl and Bell, 1997; Zeyl et al., 2003; Goddard et al., 2005). Natural *S. cerevisiae* isolates are always diploid, and they have been reported to often exhibit extremely low spore viability, which indicates the presence of haploid lethal mutations in the genome (Johnston et al., 2000). Such yeast strains would generate very few new diploid cells if they rely on diploidyzation via mother–daughter mating, because this requires at least one haploid mitotic division and leads to homozygous genomes. However, mother–daughter mating may offer an efficient way to occasionally generate diploid strains that have lost all deleterious mutations, which is a process termed renewal of the genome (Mortimer et al., 1994; Mortimer, 2000). In contrast, direct mating of spores from the same ascus after meiosis prevents haploid mitotic divisions and leads to partial reconstitution of the heterozygous stage of the genome as it was before meiosis occurred. This obviously can rescue postmeiotic genomes that are associated with a lethal mutation (Fig. 7 C). In this context, the centromere and, thus, the mating-type linkage of an overrepresented number of essential genes (Fig. 8 A) becomes plausible. It supports the idea that nonsister mating might be associated with a population genetic advantage for natural *S. cerevisiae*, which is linked to the handling of acquired disadvantageous mutations. This may indicate coevolution of this aspect of global genome organization with increased efficiency of intratetrad nonsister mating. The advantage of intratetrad mating, however, appears to be not only restricted to haploid lethal mutations, as it also provides a fitness advan-

tage to the offspring in situations where genomes, which vary by a high degree of polymorphisms, undergo meiotic mixing (Fig. 8 B). As shown recently, genetic interactions between polymorphisms are widespread and can significantly affect gene expression in yeast (Brem et al., 2005). Thus, it appears that many such interactions are, in fact, not well balanced upon the new recombination of genomes and, therefore, exhibit disadvantageous properties with consequences on the fitness of individuals. Our results also prove that the heterozygous situation can compensate for this. This suggests that many of these polymorphisms are of a recessive nature.

MP assembly: a self-organizing system able to convert a continuous signal into a digital response

We demonstrate that the regulation of spore production depends on the amounts of three proteins: Mpc54p, Mpc70p, and Spo74p. The amounts of these proteins are varied according to externally available amounts of acetate. A transcriptional control of MP component abundance is suggested by the influence of the gene dosage of MP components on the numbers of spores, but we did not rule out experimentally that there are other levels of regulation as well. It might be that protein stability or other posttranslational regulation is involved to adjust the protein concentrations or is used to fine tune the whole system. At first glance, the regulation of spore number formation by protein abundance might appear trivial; the higher the concentration of the proteins, the more spores will be obtained. Complexity is added to the system by the fact that a graded input, namely the increasing amounts of MP components, has to be translated into a digital outcome, which is the assembly of one to four MPs. This is required because exactly four haploid genomes are available for the formation of spores. The SPBs, which correspond in number precisely to the number of genomes, are part of the system. The SPBs provide spatially restricted sites. In this respect, the number of SPBs determines the possible discretization. Moreover, the system requires feedback to generate bistable behavior (Ferrell, 2002) that is necessary to flip an SPB from the off state (not involved in spore formation) to a stable on state (forms a spore). Irreversibility may be another necessary feature of the system because the trigger could be available only for a short period during the cell cycle. Additionally, the system must be able to generate the response locally on the SPBs, and this response must be communicated to other SPBs. The properties of crystal-like assemblies on the SPBs meet all of the requirements of such a system. Thereby, the binding properties of MP components to the SPBs change from exchangeable to nonexchangeable. This rationale suggests a simple, positive feedback provided by the crystal size that leads to a proportional increase in the growth rate.

Currently, we are unsure about the precise mechanism that initiates the formation of MP crystals on selected SPBs. A plausible assumption would be that a regulatory activity is enabling crystal seeding (e.g., via down-regulation of an inhibitory activity or up-regulation of a promoting activity) at a certain time point of meiosis (onset of meiosis II) and that this activity is present at different amounts on the SPBs from different generations. There must be a stochastic process involved because the age bias that directs MP assembly to specific SPBs is not followed strictly. This may relate to very initial events. The observation that the assembly of only one MP is possible with high fidelity, although it occurs on one of two SPBs from the same generation, suggests that digitization does not depend on the age bias of SPBs alone. However, it has been recently shown that not only the age of a particular SPB but also the age of the SPB next to which a new SPB is formed can influence the binding of a protein (Grallert et al., 2004). This would mean that the two new SPBs are also different. We tried to address this question experimentally but could not obtain conclusive results.

What is the role of the age bias of the SPB? Is it needed for faithful digitization of the MP assembly? We think that the age bias generates initial differences between the SPBs that are sufficiently large enough that they can become amplified during MP assembly. This would make the system more robust. Because the molecular basis of the age difference of SPBs or centrosomes is unsolved for all cases in which it was observed to influence the asymmetric localization of proteins (Pereira et al., 2001; Piel et al., 2001; Uetake et al., 2002; Grallert et al., 2004; Maekawa and Schiebel, 2004), the final answer to this question cannot be given.

Positive feedback mechanisms are able to amplify small initial asymmetries. During MP assembly, the initial event might be the formation of a crystal seed. Crystal growth then generates positive feedback because a bigger crystal offers more binding sites for new subunits. Feedback during MP assembly appears to be rather direct and proportional with the size of MP structure. However, it is possible that the MP recruits further enhancing activities in a size-dependent manner to the SPBs. This would lead to stronger feedback provided by the size of the crystal.

The simulation supports the idea that the aforementioned positive feedback circuit in combination with SPB–SPB communication via the pool of free subunits is sufficient to digitize MP assembly. The incorporation of population statistics was useful because it enabled fitting of the simulation to real data. It also enabled us to study alterations of SNC upon the introduction of mutations using quantitative predictions and subsequent validation with the sporulation profiles of the corresponding mutations. For the *Δady2* mutant, the simulation did not require changing the parameters that describe SPB–SPB differences; thus, Ady2p is predicted to function only through the regulation of the abundance of available amounts of MP components (e.g., expressional control of the MP genes *MPC54*, *MPC70*, and *SPO74*).

Is acetate-dependent regulation of protein abundance limited to the MP components? We investigated the acetate and *ADY2* dependency of protein levels of other proteins, especially components involved in the formation of early intermediates of the spores (Ady3p and Ssp1p; Moreno-Borchart et al., 2001). The levels of these proteins showed a similar acetate-dependent regulation as found for the MP components (unpublished data). These proteins have no contribution during the initiation of spore formation and MP assembly (Moreno-

Borchart et al., 2001). Therefore, the acetate-dependent regulation appears to be a more global adaptation, which, in addition to directly controlling spore number formation via protein levels of MP components, also adjusts the amounts of other proteins according to the number of formed spores. Thereby, the cell restricts the production of proteins to the amounts actually needed. Further experiments will be needed to investigate this as well as the underlying signaling processes.

SNC in other yeast species

The MP components, which provide the properties of crystal formation, are conserved within the clade of the hemiascomycete yeasts (www.yeastgenome.org). Many hemiascomycete species have been reported to form asci with variable numbers of spores (Kurtzman and Fell, 1998). In more distant fungi, such as *Schizosaccharomyces pombe*, no obvious homologues of the MP components can be found. To test whether *S. pombe* is able to regulate the production of less than four spores per ascus, we tried various starvation conditions for the sporulation of diploid *S. pombe* cells. We found no indication of SNC in this species (unpublished data). Rather, it appeared that entry into meiosis was subject to regulation, suggesting that this species regulates the spore production on another level. It remains to be answered whether any other fungi evolved a mechanism that regulates spore production in a similar way. If not, one may consider SNC as an evolutionary trait of hemiascomycete yeasts.

Materials and methods

Yeast strains

Manipulation of yeast strains (tagging with fluorescent proteins, marker insertions, gene deletions, and promoter substitution using the *CUP1-1* promoter) was performed as described previously (Janke et al., 2004). The strains generated during the course of this work are listed in Table I.

Sporulation and spore counting

Highly standardized sporulation conditions were used, and we confirmed that our protocol was able to reproduce results when performed on different days. It essentially followed the method described previously by Alani et al. (1990). In brief, the strains were thawed from glycerol −80°C stocks, grown on YP–glycerol plates for 2 d, streaked to single colonies on YPD plates, and grown for 2 d. Single colonies were used to inoculate 25 ml YPD cultures in a 100-ml flask and were grown for 30 h (230 rpm at 30°C). Presporulation growth was performed in 1% YP–acetate for 13.5 h (1:50 inoculation of 400 ml in a 2-liter flask at 230 rpm, 30°C, and good aeration). Cells were washed once with water (1 vol at RT and 2,000 rpm for 3 min) and distributed in 50-ml aliquots into 250-ml flasks with sporulation medium (water with the indicated amount of KAc [wt/vol]; added from a sterile filtered stock solution) at a cell density of 1 OD_{600} (10^7 cells/ml). Sporulation was performed without sealing the flasks for >24 h at 230 rpm and 30°C. Thereupon, aliquots of the cells were fixed with 70% ethanol, washed with water, and resuspended in 60% glycerol/water containing 1 μg/ml Hoechst 33342.

Spore counting was performed using stacks of images acquired from Hoechst 33342–stained samples. We used a microscope (IRBE; Leica) equipped with a 63× NA 1.4 oil objective (Leica), a camera (CoolSNAP HQ; Photometrics), and a DAPI filter set (Chroma Technology Corp.). The pictures were recorded using Metamorph software (Molecular Devices). Maximum projections of the Hoechst 33342 images were superimposed with the phase-contrast image using Metamorph software. G_0 and nonads (meiosis but no spores) were discriminated based on Hoechst 33342

Table I. **Strains and plasmids**

Name	Genotype	Source
YKS32	SK-1 background *lys2/lys2 ura3/ura3 LEU2/leu2::hisG ho::hisG/ho::LYS2*	(Knop and Strasser, 2000)
LH177	SK-1 background *ho::hisG/ho::hisG lys2/lys2 ura3/ura3 leu2/leu2 his3/his3 trp1/trp1*	(Huang et al., 2005)
YCT806	YKS32 background *MPC54::YFP::hphNT1/MPC54::YFP::hphNT1 SPC42::RedStar::kanMX/SPC42::RedStar::kanMX SPC110::CFP::kanMX/SPC110::CFP::kanMX*	this study
YCT851	YKS32 background *kanMX::P_{CUP1-1}::MPC54/MPC54 kanMX::P_{CUP1-1}::MPC70/MPC70 natNT2::P_{CUP1-1}::SPO74/SPO74*	this study
YCT900	YKS32 background *MPC54::GFP::kanMX/MPC54::GFP::kanMX SPC42::eqFP611::kanMX/SPC42::eqFP611::kanMX*	this study
YCT730	LH177 background *MPC54::GFP::kanMX/MPC54::GFP::kanMX*	this study
YMK470	LH177 background *MPC54::GFP::kanMX/MPC54::GFP::kanMX Δmpc70::kanMX/Δmpc70::kanMX*	(Knop and Strasser, 2000)
YCT775	YKS32 background *Δmpc54::kanMX/MPC54 Δmpc70::kanMX/MPC70 Δspo74::kanMX/SPO74*	this study
YCT815	YKS32 background *Δura3::MPC54::MPC70::kanMX/Δura3::MPC54::MPC70::kanMX Δleu2::SPO74::hphNT1/Δleu2::SPO74::hphNT1*	this study
YCT765	YKS32 background *Δady2::hphNT1/Δady2::hphNT1*	this study
YCT839	YKS32 background *Δady2::natNT2/Δady2::natNT2 Δura3::MPC54::MPC70::kanMX/Δura3::MPC54::MPC70::kanMX Δleu2::SPO74::hphNT1/Δleu2::SPO74::hphNT1*	this study
YCT925	YJM145 *HO/HO CEN5-hphNT1/CEN5*	this study
KN9268	SK-1 *HO/HO his3/his3 trp1/trp1 leu2/leu2 ura3/ura3*	K.P. Rabitsch/K. Nasmyth
YCT930	KN9268 background *HO/HO CEN5-kanMX/CEN5-hphNT1*	this study
YCT919	KN9268 background *HO/HO CEN5-hphNT1/CEN5*	this study
YCT918	KN9268 background *HO/HO CEN5-kanMX/CEN5*	his study
YCT931	Hybrid background SK-1/YJM145 *HO/HO CEN5-kanMX/CEN5-hphNT1*	this study
YCT944	KN9268 background *HO/HO CEN5-kanMX/CEN5-hphNT1 Δpre3::natNT2/PRE3*	this study
YCT945	KN9268 background *HO/HO CEN5-kanMX/CEN5-hphNT1 Δcdc5::natNT2/CDC5*	this study

staining. This spore-counting method was essential to reliably discriminate all of the different species. Counting using only phase-contrast microscopy led to significant systematic errors. Sporulation efficiency was calculated as follows: [(% tetrads × 4) + (% triads × 3) + (% dyads × 2) + % monads]/4.

Microscopic techniques

For live cell imaging, cells were adhered with Concanavalin A on small glass bottom Petri dishes (MaTek). All live cell experiments were performed at RT. Live cell imaging (Fig. 3, A and C) was performed on an imaging system (DeltaVision Spectris; Applied Precision) equipped with GFP and Cy3 filters (Chroma Technology Corp.), a 60× NA 1.4 oil immersion objective (plan Apo, IX70; Olympus), softWoRx software (Applied Precision), and a CoolSNAP HQ camera. For the experiment shown in Fig. 3 F, sporulating cells were inspected on a microscope (IRBE; Leica) equipped with a plan Apo 100× NA 1.4 oil objective (Leica), a CoolSNAP HQ camera, and DAPI, CFP, YFP, and Cy3 filter sets (Chroma Technology Corp.). FRAP was either performed on a confocal microscope (LSM 510; Carl Zeiss MicroImaging, Inc.; Fig. 4, B and C) or on a wide-field epifluorescence microscope (Axiovert 200; Carl Zeiss MicroImaging, Inc.) equipped with a laser scanner for photobleaching using a high aperture 63× NA 1.2 water immersion objective (C-Apochromat; Carl Zeiss MicroImaging, Inc.; Fig. 4 A). The wide-field microscope was necessary to visualize Mpc54p-GFP at SPBs in cells before meiosis II as a result of the lower amounts of this protein at SPBs. Quantification of videos (Figs. 3, B and D; and 4 A) was performed using MetaMorph software and maximum projections of the videos. Quantification of the experiment in Fig. 4 (B and C) was performed using LSM 510 software (Carl Zeiss MicroImaging, Inc.). Conversion of file formats from 12 to 8 bit was performed using Metamorph software. Photoshop (Adobe) was used to mount the images and to produce merged color images. No image manipulations other than contrast, brightness, and color balance adjustments were used.

For electron microscopy and analysis of the overexpression of MP genes (Fig. 4 D), a diploid strain containing one copy of *MPC54*, *MPC70*, and *SPO74* under control of the *CUP1-1* promoter (strain YCT851) was induced with 10 μm $CuSO_4$ (added 4 h after induction of sporulation on 0.3% acetate). A sample was taken at a time point in which mixed populations of cells in meiosis I and meiosis II were maximally enriched (5.5 h) and were processed for electron microscopy using osmium tetroxide fixation as described previously (Knop and Strasser, 2000). Samples were visualized on an electron microscope (Biotwin CM-120; Philips) using a CCD camera (DualVision; Gatan). Strong overexpression of all three proteins as compared with wild-type cells was validated using Western blotting.

Correlation of MP formation with the age of the SPBs involved

We fused an RFP with a retarded formation of the fluorophore of ~2–6 h (RedStar; Knop et al., 2002) to the integral SPB component Spc42p (Donaldson and Kilmartin, 1996). This allowed the discrimination of SPBs from all three generations (oldest SPB, intermediate SPB [formed before meiosis I], and two new SPBs [formed before meiosis II]; Fig. 3, E and F). (DsRed that was used previously to discriminate SPBs from different generations in yeast [Pereira et al., 2001; Nickas et al., 2004] has a maturation time of the fluorophore of >10 h and, therefore, was not suitable for this application). For live cell imaging of MP assembly, eqFP611 was used as the RFP (Janke et al., 2004). It exhibits properties similar to those of RedStar.

Immunological methods

The antibody specific for Spo74p was produced with bacterially expressed 6HIS-Spo74p and was affinity purified. All of the other antibodies have been described previously (Knop and Strasser, 2000).

Simulation of SNC

Assumptions for the digitization module (assumption A; see supplemental material) are listed as follows: (1) Initially, the free Mpc54p monomers and the Mpc70p/Spo74p heterodimers are homogeneously distributed in the cytoplasm. Diffusion is fast and readjusts a homogeneous distribution in the cytoplasm. Therefore, crystal growth is not diffusion limited. (2) The sizes of the initial crystal seeds at the four different SPBs are different. (3) Mpc54p monomers and Mpc70p/Spo74p heterodimers are incorporated into the crystals at the SPBs if they are both present in some spatial region within some short period of time. (4) A larger crystal provides more binding sites than a smaller one and, therefore, incorporates more protein. Thus, a larger crystal depletes the cytoplasmic pools more rapidly than a smaller one. (5) The crystal size is limited by the size of the SPB. (6) If the crystal size reaches a certain threshold level, the crystal is considered to be a fully functional MP.

Assumptions for the simulation of populations (sporulation profile; assumptions B and C; see supplemental material) are listed as follows: (7) The functional relationship between the number of Mpc54p, Mpc70p, and Spo74p proteins in the cell and acetate concentration (acetate → protein function) can be approximated by the experimentally derived functional relationship between sporulation efficiency and acetate concentration. (8) Because of variations within the population, the cellular response of cells in a cell population to a given acetate concentration (i.e., the amount of Mpc54p/Mpc70p/Spo70p) varies according to a second symmetric two-parameter distribution. (9) The acetate concentration available to individual cells in the population is described by a simple symmetric two-parameter distribution (e.g., Gaussian). This accounts for the asynchronicity of the population with regard to progression through meiosis. Cells that perform MP assembly earlier than others—because they performed the meiotic divisions faster—have more acetate available as a result of the simultaneous consumption of acetate by the population.

The simulations were performed using Mathematica software (version 5.0; Wolfram Research Inc.). In the first step, we designed a set of differential equations that models the crystal growth according to assumptions 1–5 (Fig. 9). To account for assumption 1, we implemented the homogeneously distributed amounts of Mpc54p monomers and Mpc70p/Spo74p heterodimers as time-dependent functions (Mpc54[t] and Mpc70Spo74[t]) that describe the available amounts of protein in the cytoplasm. We defined four time-dependent functions ($Crystal_1[t]$–$Crystal_4[t]$) that describe the crystal growth at up to four potential SPBs. To account for assumption 3, the differential equations describing the transition from spore-free to spore-containing cells contain the product of Mpc54[t] and Mpc70Spo74[t]. Assumption 4 is included by a positive feedback in the crystal growths that is proportional to the size of the corresponding crystal. Assumption 5 is implemented by a saturation function that is characterized by the two parameters of slope and maximum crystal size (saturation). The basic differential equations are shown in Fig. 9.

Initial conditions for the set of differential equations are the four different initial crystal seeds (assumption 2) and the two initial amounts of Mpc54p monomer and Mpc70p/Spo74p dimer in the cytoplasm. We calculated the initial amounts of proteins for an interval of acetate concentration using the function from assumption 7. This function (generally termed acetate → protein function, mathematically defined as Mpc54Metabolism[c] for

$$\mathrm{Mpc54'(t)} = -\mathrm{Mpc54(t)\,Mpc70Spo74(t)}\sum_{n=1}^{4}\left(1-\exp\left\{\frac{\mathrm{Slope\left(Crystal_n(t)-Saturation\right)}}{\mathrm{Saturation}}\right\}\right)\mathrm{Crystal_n(t)}$$

$$\mathrm{Mpc70Spo74'(t)} = -\mathrm{Mpc54(t)\,Mpc70Spo74(t)}\sum_{n=1}^{4}\left(1-\exp\left\{\frac{\mathrm{Slope\left(Crystal_n(t)-Saturation\right)}}{\mathrm{Saturation}}\right\}\right)\mathrm{Crystal_n(t)}$$

$$\mathrm{Crystal_n'(t)} = \mathrm{Mpc54(t)\,Mpc70Spo74(t)}\left(1-\exp\left\{\frac{\mathrm{Slope\left(Crystal_n(t)-Saturation\right)}}{\mathrm{Saturation}}\right\}\right)\mathrm{Crystal_n(t)}\Big|_{n=1..4}$$

Figure 9. **Basic differential equations derived from assumptions 1–5.** See Materials and methods.

Mpc54p monomers and Mpc70Spo74Metabolism[c] for Mpc70p/Spo74p heterodimers; see supplemental material) is characterized by three parameters: an offset, the steepness, and the maximum amplitude. The set of nonlinear differential equations was solved numerically and iteratively for the entire interval of acetate concentrations.

In the second step, we derived the steady-state crystal sizes from the numerical solution of the differential equations. Corresponding to assumption 6, all crystals with a size above a given threshold (30% of the maximum crystal size, defined by the saturation parameters) were regarded as spores. We defined SporesSum[c] as the function that represents the number of spores resulting from this digitization step depending on the acetate concentration c. Assumption 8 was implemented by convolving this function with the Gaussian distribution that describes the variation of available acetate. As a result, we obtained the statistical appearances of the five possible spore configurations (0–4 spores) depending on the acetate concentration c.

Finally, we iterated the steps of solving the differential equations and calculating the statistical appearances for a certain interval of maximum amplitudes of Mpc54Metabolism[c] and Mpc70Spo74Metabolism[c]. Considering assumption 9, the statistical appearances were weighted using the Gaussian distribution for the maximum amplitudes that are introduced to model the cellular response. This yielded the theoretical sporulation profile.

Mating assay

Different dominant markers (*hphNT1* or *kanMX4*; Janke et al., 2004) were introduced next to the centromeres of chromosome V between ORFs *YER001w* and *YER002w* in a diploid homothallic yeast strain (SK1 background; resulting strains YCT918 and YCT919). The heterozygous *CEN5-hph/CEN5-kan* strain (YCT930) was selected on Hygromycin B/G418 plates upon the mating of spores of strains YCT918 and YCT919. YCT930 was then used to delete one copy of either *CDC5* (ORF YMR001c) or *PRE3* (ORF YJL001w) with the *natNT2* marker (Janke et al., 2004). After sporulation in liquid medium containing either 0.1 or 0.01% acetate medium, 10^7 asci were spotted on a YPD plate. Unsporulated cells were killed by ether treatment (Guthrie and Fink, 1991). The ascii were incubated on YPD plates for 18 h. The cells were collected and spread on YPD plates (100–150 colonies per plate) and grown for 2 d. The colonies were assayed for the presence of all three markers simultaneously (kan+, hph+, and nat+) as well as for only two or one of the markers by replica plating. 400–600 colonies were evaluated for each sample. Colonies, which contained cells with all three markers, were considered to derive from cells (with respect to the deletion of the essential gene) that were formed by mating of nonsister spores. Cells containing the nat+ marker (which marks the deletion of the essential gene) but only the kan+ or hph+ marker in addition were considered to be the result of mating upon germination but not between nonsister spores. Colonies containing the kan+ and/or the hph+ marker but not the nat+ marker were considered to originate from other types of mating.

Fitness experiment

A homothallic YJM145/SK1 (Kane and Roth, 1974; McCusker et al., 1994) hybrid strain was generated by mating spores of strain YCT925 (YJM145 background) that contained one *CENV-hphNT1* integration with spores of strain YCT918 that contained one *CENV-kanMX* integration and selection on Hygromycin B/G418 plates. Upon sporulation of the resulting strain under low acetate concentration (0.01%), a population of heterozygous diploids was generated through the isolation of 80 dyads by micromanipulation (of which 88% did form a colony). For the generation of homozygous diploids, 40 dyads were dissected (spore survival frequency was 68%). Both species were grown on YPD plates for 2 d and independently pooled in water. Equal amounts of the cells (each 5×10^5 cells) were mixed and grown at 30°C in 400 ml YPD for 24 h (~12–13 generations). For subsequent rounds, 10^6 cells were transferred to a new flask and grown for another 12–13 generations. The composition of the culture was analyzed in the beginning of the experiment and after each round of growth for the content of hph+ or kan+ (homozygous diploids) or hph+ and kan+ cells (heterozygous diploids).

Calculation of the fraction of ORFs in the yeast genome with significant centromere linkage

Significant centromere linkage can be observed up to ~35 cM away from the centromere (Sherman and Wakem, 1991), whereas the total yeast genome covers ~4,500 cM (Mortimer et al., 1992). With 16 chromosomes present in yeast and a total of 5,792 annotated protein-encoding ORFs (www.yeastgenome.org), an estimated 1,440 ORFs are within the *CEN*-linked region.

Statistical significance of centromere linkage for groups of genes

Fig. 8 A shows that essential genes are overrepresented close to the centromeres. 70/317 genes found within a 20-kbp distance to a centromere are essential. In comparison, 1,032/5,773 yeast genes are essential. This overrepresentation of essential genes is significant at a $P = 0.03$ according to a hypergeometric test.

Online supplemental material

Videos 1 and 2 show the transition from anaphase meiosis I to metaphase meiosis II and correspond to Fig. 3 (A and C). Supplemental material provides the Mathematica files for the simulation (Fig. 6) and provides a description of the three parts of the simulation. Online supplemental material is available at http://www.jcb.org/cgi/content/full/jcb.200507168/DC1.

We would like to thank Joel Boudouin for help with FRAP experiments and Rainer Pepperkok, Jens Rietdorf, and Holger Erfle for advice with image processing. We also thank Giora Simchen, Darren Gilmour, and Eric Karsenti for discussions, Mike Strein for help during data acquisition, and Daniel DiToro for help during preparation of the manuscript.

Submitted: 29 July 2005
Accepted: 19 October 2005

References

Adams, I.R., and J.V. Kilmartin. 1999. Localization of core spindle pole body (SPB) components during SPB duplication in *Saccharomyces cerevisiae*. *J. Cell Biol.* 145:809–823.

Alani, E., R. Padmore, and N. Kleckner. 1990. Analysis of wild-type and rad50 mutants of yeast suggests an intimate relationship between meiotic chromosome synapsis and recombination. *Cell.* 61:419–436.

Bajgier, B.K., M. Malzone, M. Nickas, and A.M. Neiman. 2001. SPO21 is required for meiosis-specific modification of the spindle pole body in yeast. *Mol. Biol. Cell.* 12:1611–1621.

Bell, G. 1982. The Masterpiece of Nature: The Evolution and Genetics of Sexuality. University of California Press, Berkeley, CA. 635 pp.

Brem, R.B., J.D. Storey, J. Whittle, and L. Kruglyak. 2005. Genetic interactions between polymorphisms that affect gene expression in yeast. *Nature.* 436:701–703.

Bullitt, E., M.P. Rout, J.V. Kilmartin, and C.W. Akey. 1997. The yeast spindle pole body is assembled around a central crystal of Spc42p. *Cell.* 89:1077–1086.

Cherry, J.M., C. Ball, S. Weng, G. Juvik, R. Schmidt, C. Adler, B. Dunn, S. Dwight, L. Riles, R.K. Mortimer, and D. Botstein. 1997. Genetic and physical maps of *Saccharomyces cerevisiae*. *Nature.* 387:67–73.

Davidow, L.S., L. Goetsch, and B. Byers. 1980. Preferential occurence of nonsister spores in two-spored asci of *Saccharomyces cerevisiae*: evidence for regulation of spore-wall formation by the spindle pole body. *Genetics.* 94:581–595.

Donaldson, A.D., and J.V. Kilmartin. 1996. Spc42p: a phosphorylated component of the *S. cerevisiae* spindle pole body (SPD) with an essential function during SPB duplication. *J. Cell Biol.* 132:887–901.

Ferrell, J.E., Jr. 2002. Self-perpetuating states in signal transduction: positive feedback, double-negative feedback and bistability. *Curr. Opin. Cell Biol.* 14:140–148.

Goddard, M.R., H.C. Godfray, and A. Burt. 2005. Sex increases the efficacy of natural selection in experimental yeast populations. *Nature.* 434:636–640.

Grallert, A., A. Krapp, S. Bagley, V. Simanis, and I.M. Hagan. 2004. Recruitment of NIMA kinase shows that maturation of the *S. pombe* spindle-pole body occurs over consecutive cell cycles and reveals a role for NIMA in modulating SIN activity. *Genes Dev.* 18:1007–1021.

Guilliermond, M.A. 1905. Recherches sur la germination des spores et la conjugation chez les levures. *Rev. Gen. Bot.* 509:337–376.

Guthrie, C., and G. Fink, editors. 1991. Methods in Enzymology: Guide to Yeast Genetics and Molecular Biology. Vol. 194. Academic Press Inc., London. 735 pp.

Hawthorne, D.C., and R.K. Mortimer. 1960. Chromosome mapping in *Saccharomyces*: centromere-linked genes. *Genetics.* 45:1085–1110.

Herskowitz, I. 1988. Life cycle of the budding yeast *Saccharomyces cerevisiae*. *Microbiol. Rev.* 52:536–553.

Huang, L.S., H.K. Doherty, and I. Herskowitz. 2005. The Smk1p MAP kinase negatively regulates Gsc2p, a 1,3-beta-glucan synthase, during spore wall morphogenesis in *Saccharomyces cerevisiae*. *Proc. Natl. Acad. Sci. USA.* 102:12431–12436.

Ishihara, S., A. Hirata, M. Minemura, S. Nogami, and Y. Ohya. 2001. A muta-

tion in SPC42, which encodes a component of the spindle pole body, results in production of two-spored asci in *Saccharomyces cerevisiae*. *Mol. Genet. Genomics.* 265:585–595.

Janke, C., M.M. Magiera, N. Rathfelder, C. Taxis, S. Reber, H. Maekawa, A. Moreno-Borchart, G. Doenges, E. Schwob, E. Schiebel, and M. Knop. 2004. A versatile toolbox for PCR-based tagging of yeast genes: new fluorescent proteins, more markers and promoter substitution cassettes. *Yeast.* 21:947–962.

Johnston, J.R., C. Baccari, and R.K. Mortimer. 2000. Genotypic characterization of strains of commercial wine yeasts by tetrad analysis. *Res. Microbiol.* 151:583–590.

Kane, S.M., and R. Roth. 1974. Carbohydrate metabolism during ascospore development in yeast. *J. Bacteriol.* 118:8–14.

Kassir, Y., N. Adir, E. Boger-Nadjar, N.G. Raviv, I. Rubin-Bejerano, S. Sagee, and G. Shenhar. 2003. Transcriptional regulation of meiosis in budding yeast. *Int. Rev. Cytol.* 224:111–171.

Kilmartin, J.V., S.L. Dyos, D. Kershaw, and J.T. Finch. 1993. A spacer protein in the *Saccharomyces cerevisiae* spindle pole body whose transcript is cell cycle-regulated. *J. Cell Biol.* 123:1175–1184.

Kirby, G.C. 1984. Breeding systems and heterozygosity in populations of tetrad forming fungi. *Heredity.* 52:35–41.

Knop, M., and K. Strasser. 2000. Role of the spindle pole body of yeast in mediating assembly of the prospore membrane during meiosis. *EMBO J.* 19:3657–3667.

Knop, M., F. Barr, C.G. Riedel, T. Heckel, and C. Reichel. 2002. Improved version of the red fluorescent protein (drFP583/DsRed/RFP). *Biotechniques.* 33:592, 594, 596–598 passim.

Knop, M., K.J. Miller, M. Mazza, D. Feng, M. Weber, S. Keranen, and J. Jantti. 2005. Molecular interactions position Mso1p, a novel PTB domain homologue, in the interface of the exocyst complex and the exocytic SNARE machinery in yeast. *Mol. Biol. Cell.* 16:4543–4556.

Kurtzman, C.P., and J.W. Fell, editors. 1998. The Yeasts: a Taxonomic Study. Elsevier Science Publishing Co. Inc., Amsterdam. 1055 pp.

Mable, B.K., and S.P. Otto. 2001. Masking and purging mutations following EMS treatment in haploid, diploid and tetraploid yeast (*Saccharomyces cerevisiae*). *Genet. Res.* 77:9–26.

Maekawa, H., and E. Schiebel. 2004. Cdk1-Clb4 controls the interaction of astral microtubule plus ends with subdomains of the daughter cell cortex. *Genes Dev.* 18:1709–1724.

McCusker, J.H., K.V. Clemons, D.A. Stevens, and R.W. Davis. 1994. Genetic characterization of pathogenic *Saccharomyces cerevisiae* isolates. *Genetics.* 136:1261–1269.

Moreno-Borchart, A.C., and M. Knop. 2003. Prospore membrane formation: how budding yeast gets shaped in meiosis. *Microbiol. Res.* 158:83–90.

Moreno-Borchart, A.C., K. Strasser, M.G. Finkbeiner, A. Shevchenko, and M. Knop. 2001. Prospore membrane formation linked to the leading edge protein (LEP) coat assembly. *EMBO J.* 20:6946–6957.

Mortimer, R.K. 2000. Evolution and variation of the yeast (*Saccharomyces*) genome. *Genome Res.* 10:403–409.

Mortimer, R.K., C.R. Contopoulou, and J.S. King. 1992. Genetic and physical maps of S*accharomyces cerevisiae*, Edition 11. *Yeast.* 8:817–902.

Mortimer, R.K., P. Romano, G. Suzzi, and M. Polsinelli. 1994. Genome renewal: a new phenomenon revealed from a genetic study of 43 strains of *Saccharomyces cerevisiae* derived from natural fermentation of grape musts. *Yeast.* 10:1543–1552.

Nickas, M.E., C. Schwartz, and A.M. Neiman. 2003. Ady4p and Spo74p are components of the meiotic spindle pole body that promote growth of the prospore membrane in *Saccharomyces cerevisiae*. *Eukaryot. Cell.* 2:431–445.

Nickas, M.E., A.E. Diamond, M.J. Yang, and A. Neiman. 2004. Regulation of spindle pole function by an intermediary metabolite. *Mol. Biol. Cell.* 15:2606–2616.

Okamoto, S., and T. Iino. 1981. Selective abortion of two nonsister nuclei in a developing ascus of the hfd-1 mutant in *Saccharomyces cerevisiae*. *Genetics.* 99:197–209.

Paiva, S., F. Devaux, S. Barbosa, C. Jacq, and M. Casal. 2004. Ady2p is essential for the acetate permease activity in the yeast *Saccharomyces cerevisiae*. *Yeast.* 21:201–210.

Palkova, Z., F. Devaux, M. Icicova, L. Minarikova, S. Le Crom, and C. Jacq. 2002. Ammonia pulses and metabolic oscillations guide yeast colony development. *Mol. Biol. Cell.* 13:3901–3914.

Pereira, G., T.U. Tanaka, K. Nasmyth, and E. Schiebel. 2001. Modes of spindle pole body inheritance and segregation of the Bfa1p-Bub2p checkpoint protein complex. *EMBO J.* 20:6359–6370.

Piel, M., J. Nordberg, U. Euteneuer, and M. Bornens. 2001. Centrosome-dependent exit of cytokinesis in animal cells. *Science.* 291:1550–1553.

Rabitsch, K.P., A. Toth, M. Galova, A. Schleiffer, G. Schaffner, E. Aigner, C. Rupp, A.M. Penkner, A.C. Moreno-Borchart, M. Primig, et al. 2001. A screen for genes required for meiosis and spore formation based on whole-genome expression. *Curr. Biol.* 11:1001–1009.

Riedel, C.G., M. Mazza, P. Maier, R. Korner, and M. Knop. 2005. Differential requirement for phospholipase D/SPO14 and its novel interactor SMA1 for regulation of exocytotic vesicle fusion in yeast meiosis. *J. Biol. Chem*. doi:10.1074/jbc.M504244200.

Schneper, L., K. Duvel, and J.R. Broach. 2004. Sense and sensibility: nutritional response and signal integration in yeast. *Curr. Opin. Microbiol.* 7:624–630.

Sherman, F., and P. Wakem. 1991. Mapping yeast genes. *Methods Enzymol.* 194:38–57.

Shimoda, C. 2004. Forespore membrane assembly in yeast: coordinating SPBs and membrane trafficking. *J. Cell Sci.* 117:389–396.

Taxis, C., and M. Knop. 2004. Regulation of exocytotic events by centrosome-analogous structures. *Topics Curr. Gen.* 10:193–207.

Uetake, Y., K.H. Kato, S. Washitani-Nemoto, and S. Nemoto Si. 2002. Non-equivalence of maternal centrosomes/centrioles in starfish oocytes: selective casting-off of reproductive centrioles into polar bodies. *Dev. Biol.* 247:149–164.

Wesp, A., S. Prinz, and G.R. Fink. 2001. Conservative duplication of spindle poles during meiosis in *Saccharomyces cerevisiae*. *J. Bacteriol.* 183:2372–2375.

Winge, O., and O. Laustsen. 1937. On two types of spore germination and on genetic segregations in *Saccharomyces*, demonstrated through single-spore cultures. *C.R. Trav. Lab. Carlsberg Ser. Physiol.* 22:99–117.

Zakharov, I.A. 1968. Homozygousity in intratetrad and intraoctad fertilization in fungi. *Genetika.* 4:98–105.

Zeyl, C., and G. Bell. 1997. The advantage of sex in evolving yeast populations. *Nature.* 388:465–468.

Zeyl, C., T. Vanderford, and M. Carter. 2003. An evolutionary advantage of haploidy in large yeast populations. *Science.* 299:555–558.